

行政院國家科學委員會專題研究計畫成果報告

金屬陽離子在二氧化矽／水溶液固液界面反應之研究

Interaction of metallic cations between the interface of
 $\text{SiO}_{2(s)}$ /solution.

計畫編號：NSC 89-2211-E-002-018

執行期限：88 年 8 月 1 日至 89 年 7 月 31 日

主持人：駱尚廉教授(s11o@ccms.ntu.edu.tw) 台大環工所

研究生：官文惠(d4541005@ms.cc.ntu.edu.tw)台大環工所

一、中文摘要

不論在自然界之河川、湖泊水體、底泥，或在污泥堆置、廢棄物掩埋場之土壤、地下水層中，金屬陽離子之傳輸與流佈均是環境工程所關切之問題。惟其行為常受周遭固相介質之影響，而在固/液界面發生吸附、水解、表面沈澱等反應。事實上，從吸附到水解以至於表面沈澱應是一個連續的過程。金屬陽離子會隨著液相濃度、pH 值以及反應時間之提高，而在固相表面發生吸附、水解最後形成表面新沈澱固相之反應。二氧化矽是地殼中含量最豐富的礦物也是此工業上廣泛應用的基材，故本研究將以二氧化矽為固相氧化物，探討三價鋁及三價鐵兩種金屬陽離子於不同系統 pH 值、不同金屬陽離子濃度下，在其表面與水溶液間之反應。

穿透式電子顯微鏡觀察結果顯示純二氧化矽系統之顆粒會聚集在一起。三價鐵/二氧化矽系統會有不連續的氫氧化鐵固體物出現在液相中。三價鋁/二氧化矽系統不論在高的系統 pH 值下，其金屬氫氧化物固體會在原二氧化矽表面開始成長。

在電泳動實驗顯示，當二氧化矽表面吸附/沈澱金屬陽離子時表面電性會發生改變。亦即系統有三次的電性逆轉點。當表面還未吸附金屬陽離子時，呈現原二氧化矽之特性，即電性逆轉點 1；電性逆轉點 2 表示開始發生表面沈澱現象；電性逆轉點 3 則為金屬陽離子氫氧化物固體之等電點值。

關鍵詞：二氧化矽、三價鋁、三價鐵、表面反應、穿透式顯微鏡、電泳

Abstract

The transport and fate of metallic cations are issues of concern with regard to the natural environment, such as rivers, lakes, groundwater, and soil in waste disposal sites. When cations exist in an oxide suspension system, it has been proposed that a transition takes place from mononuclear adsorption to hydrolysis to multinuclear adsorption and, finally, to precipitation on the oxide surface or in bulk solution with increasing system pH or cation concentration. SiO_2 is the most abundant oxide in the earth crust and can significantly influence a variety of nutrients and pollutants in aquatic and soil environments. Moreover, SiO_2 is widely applied to many industrial processes including use as filtration medium in water treatment plants and base substrate in catalysts. Thus, the objectives of this study are to explore the interaction of various metallic cations (Al(III) and Fe(III)) between the interface of SiO_2 and aqueous solution.

The TEM images show that pure silica particles are aggregate and that the diameter of a primary particle is around 15-25 nm. It is obviously shown from the results that discrete Fe(OH)_3 precipitate forms both at low pH (2.40) and at high pH (7.00) around the unchanged size of base SiO_2 particle. However, no discrete Al(OH)_3 phase is evident in the $\text{Al(III)}/\text{SiO}_2$ systems. The invisibility of discrete Al(OH)_3 precipitate suggests a strong association between Al-hydroxide and the SiO_2 surface. With an increasing system pH, the Al(OH)_3 precipitate gradually forms on the surface of

the base SiO_2 particle and the particle size becomes larger.

The charge reversals (CR) observed in the $\text{Al(III)}/\text{SiO}_2$ system represent, in order of increasing pH, the point-of-zero charge (PZC) on the SiO_2 substrate (CR1), the pH of surface nucleation of Al(OH)_3 (CR2), and, at high pH, the PZC of the Al(OH)_3 coating (CR3). The observed electrophoresis mobility of $\text{Fe(III)}/\text{SiO}_2$ is the overall result contributed by negatively charged SiO_2 and positively charged Fe(OH)_3 .

Keywords: SiO_2 , Al(III) , Fe(III) , Surface reactions, TEM, Electrophoresis

二、Motivation and Objectives

When cations exist in an oxide suspension system, it has been proposed that a transition takes place from mononuclear adsorption to hydrolysis to multinuclear adsorption, and finally, to precipitation on the oxide surface or in bulk solution with increasing system pH (Chisholm-Brause *et al.*, 1990; Katz and Hayes, 1995a; 1995b). The bulk and surface characteristics of these mixed oxides are fundamental parameters in determining the distribution of a variety of nutrients and pollutants in the environment (Anderson and Benjamin, 1990a). An understanding of when and how such a transition forms is important in a number of areas that are of scientific and technological importance (Towle *et al.*, 1997). For instance, an understanding of the process is required for accurate quantitative modeling of metal ion uptake (Sposito, 1984; Stumm and Wieland, 1990). The morphology and distribution of the final precipitates are critical factors in certain technological applications, such as the preparation of heterogeneous catalysts and the formation of coatings.

A substantial amount of research has demonstrated that minerals, such as the oxides of Al, Fe and Si, can significantly influence the distribution, mobility, and bioavailability of trace elements in aquatic environments (Reid and McDuffie, 1981; Millward and Moore, 1982; Anderson and

Benjamin, 1990a). Most of this research, however, focused on relatively well-defined solids. In natural aquatic environments, reactions such as colloidal adhesion, dissolution, adsorption and precipitation in bulk solution or on oxide surface can create multicomponent solids with bulk and surface properties different from the base pure solids. Although there have been several studies of adsorption onto multicomponent solids (Anderson and Benjamin, 1990b; Crawford *et al.*, 1993; Meng and Letterman, 1993; Karthikeyan *et al.*, 1997), most of these studies briefly describe the bulk and surface properties of the solid phase instead of exploring differences of the solid phase prepared at various pH. The purpose of this study was to determine bulk and surface properties of $\text{Al(III)}/\text{SiO}_2$ and $\text{Fe(III)}/\text{SiO}_2$ suspensions with increasing pH.

三、Results and DIscussions

TEM images

Fig. 1 shows TEM image of pure silica particle aggregates. The diameter of the primary SiO_2 particle is 15-25 nm. Figs. 2a and 2b are the morphologies of SiO_2 with 1 mM of Fe(III) at pH 2.40 and pH 7.00, respectively. It is obviously shown that discrete Fe(OH)_3 precipitate formed both at low pH (2.40) and at high pH (7.00) around the unchanged size of base SiO_2 particle, and the precipitate formed at low pH was further away from the base SiO_2 particle than that prepared at high pH. Figs. 3a and 3b display the micrographs of SiO_2 with 1 mM of Al(III) at pH 3.00 and pH 5.00, respectively. No discrete Al(OH)_3 phase was evident in the $\text{Al(III)}/\text{SiO}_2$ system. Fig. 3a shows that the size of particles prepared at pH 3.00 in $\text{Al(III)}/\text{SiO}_2$ system is close to that of the base particle. Although the size of the particle prepared at pH 5.00 seemed to be slightly larger than that of the base particle, there was no discrete Al(OH)_3 phase observed. The invisibility of discrete Al(OH)_3 precipitate in the Al/SiO_2 system suspensions suggests a strong association between Al-oxide and the SiO_2 surface. With an increasing system pH, the Al(OH)_3 precipitate gradually forms on

the surface of the base SiO_2 particle and the particle size becomes larger. On the other hand, since the hydrolysis of Fe(III) occurs at low pH (~2) (Bases and Mesmer, 1976), Fe(OH)_3 could form in the bulk solution without other solid surfaces to reduce the potential energy of oxide formation (James and Healy, 1972; Bleam and McBride, 1985).

XRD and specific surface area

X-ray diffractograms of particles prepared at various pH and cations always showed X-ray non-crystalline materials (diffraction pattern not shown). These results indicate that there is no evident effect of system pH on the mineral patterns both for Al- and Fe-oxide system. The specific surface areas of the particles are listed in Table 1. The measured surface area of the SiO_2 is in good agreement with that reported by the manufacturer ($200 \pm 25 \text{ m}^2/\text{g}$). When 1 mM Fe(III) was added to 1 g of SiO_2 , no obvious change in the surface area was observed both at low (2.40) system pH and high (7.00) system pH. In 1 mM Al(III)/ SiO_2 system, the specific surface area of particles prepared at low (3.00) pH is very similar to that of the base SiO_2 particle but that of particles prepared at high (5.00) pH is slightly lower than the primary particle's.

Electrophoretic mobility

The electrophoretic mobility (EM) of pure SiO_2 suspensions over a range of pH and in three different salt solutions is shown in Fig. 4. The pH of zero particle mobility, which is referred to as the isoelectric point (IEP), is 2.00 for a SiO_2 particle. In all experiments, 0.1 N KNO_3 was used as the background electrolyte. Fig. 5 shows EM data of SiO_2 suspension with various Al(III) concentrations as a function of pH. The electrophoretic behavior of SiO_2 with 1×10^{-5} M and 1×10^{-4} M of Al(III) is similar to that of pure SiO_2 suspension. While there are three charge reversal (CR) points (i.e., strictly, the pH of reversal of the electrokinetic potential) listed as CR1 (+ → -), CR2 (- → +) and CR3 (+ → -) in order of increasing pH for the curves of SiO_2 with 1×10^{-3} M, 5×10^{-3} M and 1×10^{-2} M of Al(III). The general features of these electrokinetic curves showing charge reversal are depicted

schematically in Fig. 6.

These experiments do not indicate any significant shift in CR1 at various concentrations of Al(III). The significance of CR1 is clear in that H^+ and OH^- ions are potential determining for oxides; thus CR1 is the point-of-zero charge (PZC) of the SiO_2 suspension. There is now ample evidence that, at high pH charge reversal, CR3 reflects a coating of the metal hydroxide on the colloid substrate (James and Healy, 1972). If sufficient metal ion is adsorbed to yield a complete coating of adsorbed metal hydroxide, then CR3 is the point-of-zero charge of the metal hydroxide. Incomplete coating due to low concentrations of metal or to high concentrations of colloidal substrate particles will reflect a dual surface-coated and uncoated areas. Thus, CR3 will occur at pH values at or below the pH_{pzc} of the Al(OH)_3 depending on the coverage achieved. According to Fig. 5, CR3 is made to approach the pH_{pzc} of amorphous Al(OH)_3 (~9.0) (Parks, 1965) by increasing the Al(III) concentration. The CR3 of the colloid in the 1×10^{-2} M of Al(III)/g of SiO_2 suspension is the same as the pH_{pzc} of pure Al(OH)_3 , which suggests that Al(OH)_3 has completely covered the SiO_2 particles. In Fig. 5, CR2 of the curves of SiO_2 with 1×10^{-3} M, 5×10^{-3} M and 1×10^{-2} M of Al(III) range from pH 2 to 4 and increase as the concentration of Al(III) decreases. James and Healy (1972) suggested that CR2 could indicate a surface precipitation induced at a pH below bulk precipitation. Since the interface is a region where the electric field is large and of the order of 10^6 v cm^{-1} , or more (Booth, 1951; Andersen and Bockris, 1964; James and Healy, 1972), this field will lower the dielectric constant of the interfacial medium well below that of the bulk aqueous solution. Then the change in standard free energy ($\Delta G'$) for the process of Al(OH)_3 dissolution in the SiO_2 surface can be expressed as

$$-\Delta G' \doteq -\Delta G - (G_{\text{Al}}^{3+} + G_{\text{OH}}^-) \quad [1]$$

where $\Delta G'$ is the change in free energy for the dissolution of Al(OH)_3 in bulk solution, and G_{Al}^{3+} and G_{OH}^- are the excess contribution (due to the surface-induced

electric field) to the standard free energy of individual Al^{3+} and OH^- ion, respectively. Also, Eq[1] can be represented in the form of the solubility product of Al(OH)_3 :

$$\log(K_{\text{Al(OH)}_3}/K'_{\text{Al(OH)}_3}) = (G'_{\text{Al}^{3+}} + G'_{\text{OH}^-})/2.3RT \quad [2]$$

where $K_{\text{Al(OH)}_3}$ and $K'_{\text{Al(OH)}_3}$ are the solubility product of Al(OH)_3 in the bulk solution and in the interface, respectively. According to Born charging equation (Andersen and Bockris, 1964), $G'_{\text{Al}^{3+}}$ and G'_{OH^-} are positive quantities, that is,

$$K_{\text{Al(OH)}_3} > K'_{\text{Al(OH)}_3} \quad [3]$$

Therefore, the electric field of the surface-induced precipitation in the interface will occur before the formation of bulk precipitation even though the solution is unsaturated with respect to this precipitate solid. CR2 could indicate the pH of surface precipitation induced at a pH below bulk precipitation and will shift to a lower pH with increasing Al(III) concentration.

In contrast to the Al(III)/ SiO_2 system, the EM measurements for the Fe(III)/ SiO_2 system (Fig. 7) show a negligible increase in CR3 with increasing Fe(III) concentration. CR3 is always 4.5 which is much lower than the pH_{pzC} of amorphous Fe(OH)_3 (~7.0) (Parks, 1965) even though the Fe(III) concentration increases. The TEM results (Fig. 3) indicate that the Fe(OH)_3 particle formed in the bulk solution. Therefore, the observed EM of Fe(III)/ SiO_2 is the overall result contributed by negatively charged SiO_2 and positively charged Fe(OH)_3 . Also, there is no the process of CR1 to CR2 in the EM measurements of the Fe(III)/ SiO_2 system probably because of the small value of $K_{\text{Fe(OH)}_3}$. It also means that the occurrence of Fe(III) hydrolysis at a low pH (~2) results in the overlap of CR2 with CR1.

四、成果自評

本研究成果以達成計畫內容，並已將研究內容分別發表於 *Water Science and Technology* (2000 in press) 與 *Chemosphere* **41**, 1741-

1747 (2000)兩國際期刊內。

五、REFERENCES

- Andersen T. N. and Bockris J. O'M. (1964). Forces involved in the "specific" adsorption of ions on metals from aqueous solution. *Electrochim. Acta*, 9(4), 347-371.
- Anderson P. R. and Benjamin M. M. (1990a). Surface and bulk characteristics of binary oxide suspension. *Environ. Sci. Technol.*, 24(5), 692-698.
- Anderson P. R. and Benjamin M. M. (1990b). Modeling adsorption in aluminum-iron binary oxide suspensions. *Environ. Sci. Technol.*, 24(10), 1586-1592.
- Baes C. F., Mesmer R. E. (1976). *The hydrolysis of Cations*. John Wiley & Sons, New York.
- Bleam W. F. and McBride M. B. (1985). Cluster formation versus isolated-site adsorption. A study of Mn(II) and Mg(II) adsorption on boehmite and goethite. *J. Colloid Interface Sci.*, 103(1), 124-132.
- Booth F. (1951). The dielectric constant of water and the saturation effect. *J. Chem. Phys.*, 19(4), 391-394; 19(10), 1327-1328; 19(12) 1615.
- Chisholm-Brause C. J., O'Day P. A., Brown G. E., Jr. and Parks G. A. (1990). Evidence for multinuclear metal-ion complexes at solid-water interfaces from X-ray absorption spectroscopy. *Nature*, 348, 528-530.
- Crawford R. J., Harding I. H. and Mainwaring D. E. (1993). Adsorption and coprecipitation of multiple heavy metal ions onto the hydrated oxides of iron and chromium. *Langmuir*, 9(11), 3057-3062.
- James R. O. and Healy T. W. (1972). Adsorption of hydrolyzable metal ions at the oxide-water interface. *J. Colloid Interface Sci.*, 40(1), 42-80.
- Karthikeyan K. G., Elliott H. A. and Cannon F. S. (1997). Adsorption and coprecipitation of copper with the hydrous oxides of iron and aluminum. *Environ. Sci. Technol.*, 31(10), 2721-2725.
- Katz L. E. and Hayes K. F. (1995a). Surface complexation modeling I. strategy for modeling monomer complex formation at

- moderate surface coverage. *J. Colloid Interface Sci.*, 170(2), 477-490.
- Katz L. E. and Hayes K. F. (1995b). Surface complexation modeling I. strategy for modeling polymer and precipitation reactions at high surface coverage. *J. Colloid Interface Sci.*, 170(2), 491-501.
- Meng X. and Letterman R. D. (1993). Modeling ion adsorption on aluminum hydroxide modified silica. *Environ. Sci. Technol.*, 27(9), 1924-1929.
- Millward G. E. and Moore R. M. (1982). The adsorption of Cu, Mn and Zn by iron oxyhydroxide in model estuarine solutions. *Water Res.*, 16(6), 981-985.
- Parks G. A. (1965). The isoelectric points of solid oxides, solid hydroxides, and aqueous hydroxo complex systems. *Chem. Rev.*, 65(2), 177-198.
- Reid J. D. and McDuffie B. (1981). Sorption of the trace cadmium on clay minerals and river sediments: effects of pH and Cd(II) concentrations in a synthetic river water. *Water, Air, Soil Pollut.*, 15(3), 375-386.
- Sposito G. (1984) *The Surface Chemistry of Soils*. Oxford University Press, New York.
- Stumm W. and Wieland E. (1990). Dissolution of oxide and silicate minerals: rates depend on surface speciation. In: *Aquatic Chemical Kinetics*, W. Stumm (ed.), Wiley-Interscience, pp. 367-400.
- Towle N. T., Bargar J. R., Brown Jr. G. E. and Parks G. A. (1997). Surface precipitation of Co(II) (aq) on Al₂O₃. *J. Colloid Interface Sci.*, 187(1), 62-82.

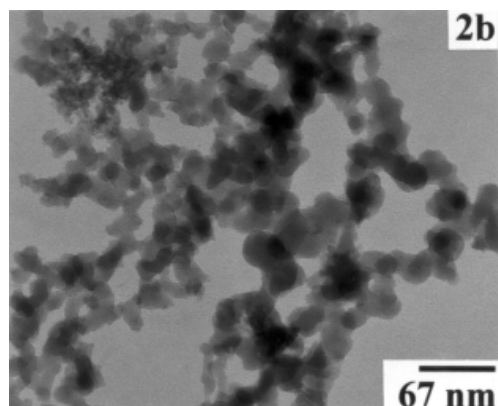
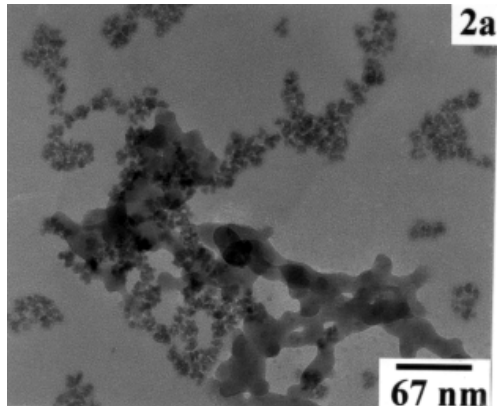


Fig. 2 TEM micrographs of Fe(III)/SiO₂ suspensions (a) prepared at pH 2.40 and (b) prepared at pH 7.00.

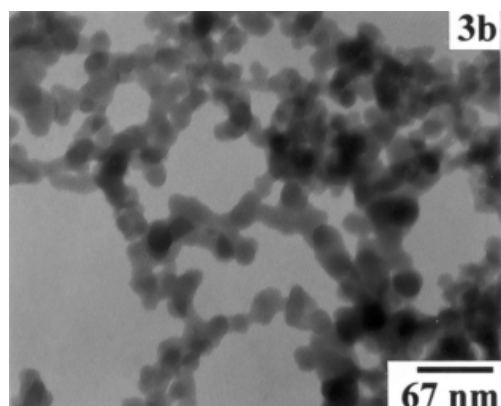
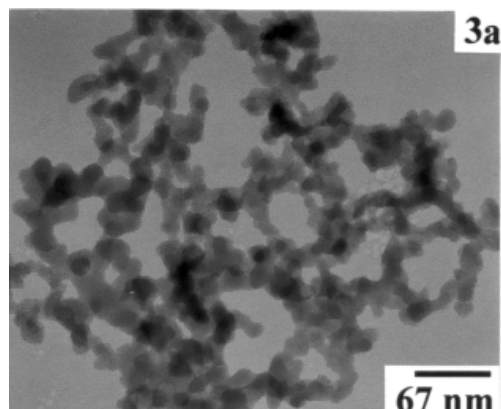


Fig. 1 TEM micrograph of base SiO₂ suspension.

Fig. 3 TEM micrographs of Al(III)/SiO₂ suspensions (a) prepared at pH 3.00 and (b) prepared at pH 5.00.

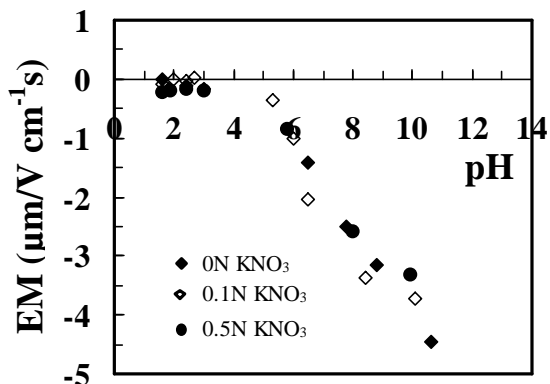


Fig. 4 The EM of SiO₂ particles as a function of pH in three concentrations of KNO₃: 0, 0.1 and 0.5 N.

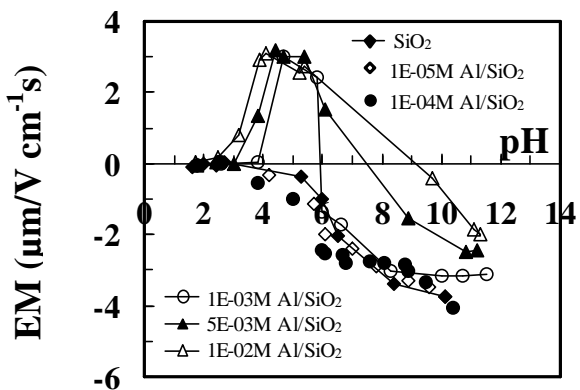


Fig. 5 The EM of Al(III)/SiO₂ suspensions as a function of pH in 0.1 N KNO₃ electrolyte with and without the presence of various concentrations of Al(NO₃)₃.

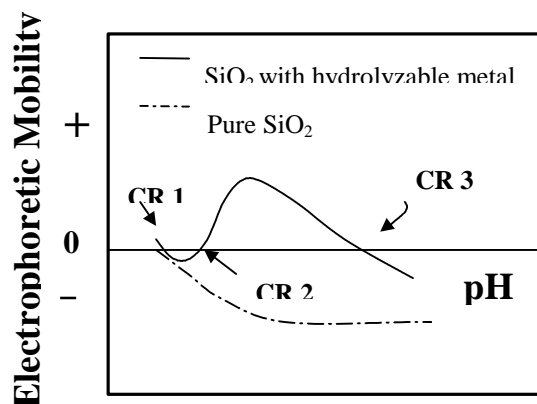


Fig. 6 Schematic illustration of the general EM behavior of colloid systems in the presence and absence of hydrolyzable metal ions.

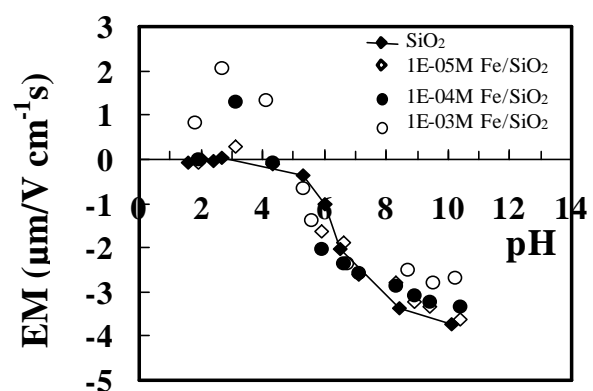


Fig. 7 The EM of Fe(III)/SiO₂ suspensions as a function of pH in 0.1 N KNO₃ electrolyte with and without the presence of various concentrations of Fe(NO₃)₃.

Table 1. Specific surface area of base SiO₂, Al(III)/SiO₂ and Fe(III)/SiO₂ particles.

pH	Base SiO ₂	Fe(III)/SiO ₂	Al(III)/SiO ₂	
	2.40	7.00	3.00	5.00
SSA(m ² /g)	204	172	200	197
			150	

